Chapter I

Introduction

1.1. Cancer

Cancer is the uncontrolled growth and spread of abnormal cells.[1,2] Cancer arises from genetic mutations that disrupt the standard regulatory mechanisms governing cell division, apoptosis, and DNA repair.[1-4] These mutations can be caused by a variety of factors, including inherited genetic predispositions, environmental exposures, and lifestyle choices.[1-4] When the regulatory mechanisms fail, cells begin to divide uncontrollably, forming masses of tissue known as tumors (Figure 1.1).[1-4] Tumors can be benign, meaning these are localized and do not invade surrounding tissues. But malignant tumors, which are cancerous, can spread to other parts of the body through a process called metastasis.[5-7] Metastasis occurs when cancer cells break away from the primary tumor, travel through the bloodstream or lymphatic system, and establish new tumors in distant organs.[5-7] This ability to spread makes cancer particularly dangerous and challenging to treat.[5-7] The progression of cancer is typically categorized into stages, ranging from Stage 0 (carcinoma *in situ*, where abnormal cells are present but not invasive) to Stage IV (advanced cancer with metastasis to distant organs).[8,9] Understanding the biological basis of cancer is crucial for developing effective treatments and improving patient outcomes.[8,9]

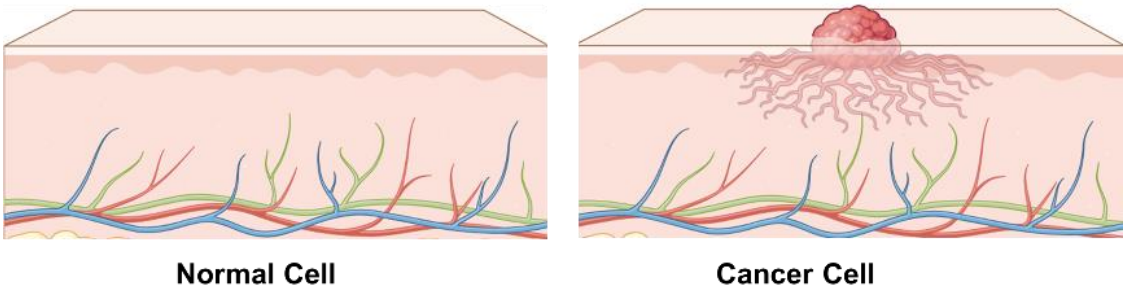

Figure 1.1: A pictorial representation of normal cells and cancerous cells.

1.2. Cancer Cases Worldwide Statistics

In the past few decades, cancer has been one of the leading causes of death worldwide, accounting for nearly 10 million deaths in 2020 alone (as per the World Health Organization, WHO, report).[10] According to GLOBOCAN data, some types of cancers cause more deaths than others.[10] Cancer does not affect all people or places in the same way.[10] For example, lung cancer is the leading cause of cancer deaths around the world, causing about 1.8 million deaths (18%). It is followed by colorectal cancer (9.4%), liver cancer (8.3%), stomach cancer (7.7%), and breast cancer (6.9%).[10]

Cancer death rates also vary by region. In high-income countries like those in Europe, the USA, Japan, and Canada, early detection, regular screening, and better treatment have helped to reduce the number of cancer deaths in recent years.[10] But in low- and middle-income countries like India and many Asian and African countries, cancer death rates remain high.[10] This is mostly because of limited access to healthcare, late diagnosis, and low awareness about how to prevent cancer.[10] In terms of new cancer cases, about 58.3% of all newly diagnosed cancers worldwide were reported in Asia, while European countries accounted for only 22.8% of new cases.[10] Gender disparities exist as well (Figures 1.2a, b), with men (Figure 1.2a) being more likely to develop and die from cancer than women (Figure 1.2b).[10] Socioeconomic status further influences cancer outcomes, as individuals with lower income and education levels often face barriers to accessing timely and effective care.[10] These statistics highlight the need for global efforts to address disparities in cancer prevention, diagnosis, and treatment.

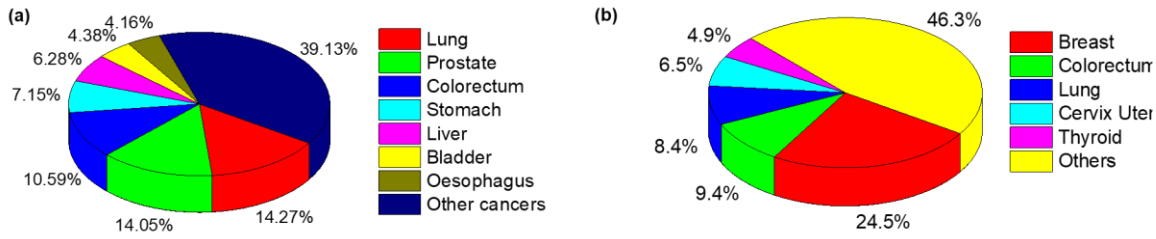

Figure 1.2: (a) Worldwide estimated number of new cancer cases in males in 2020. (b) Worldwide, the estimated number of new cancer cases in females in 2020.[10]

1.3. Various Treatment Modalities Used in Cancer Treatment

Cancer treatment involves various modalities such as surgery, radiation therapy, chemotherapy, photodynamic therapy (PDT) etc.[11-13] Surgery, radiation therapy, and chemotherapy are the most common therapies (Figure 1.3).[12-20] Each of these therapies cures cancer through different mechanisms and has its own limitations. Like, surgery is often used for localized tumors and can be curative if the cancer has not spread, but it is ineffective for metastatic cases.[16,17] Chemotherapy uses cytotoxic drugs to kill rapidly dividing cells and is effective

Figure 1.3: Major Cancer therapies. (Adapted from www.theayurveda.org, https://www.usf.edu, https://www.thenewsminute.com, https://www.bswhealth.com).

for systemic cancers. However, despite the clinical success, several limitation poses significant challenges to chemotherapy, such as drug resistance issues, poor selectivity, various side effects like autotoxicity, nephrotoxicity, neurotoxicity, hepatotoxicity, vomiting, nausea, etc.[12,14,15] Whereas, radiation therapy uses high-energy γ-rays to destroy cancer cells. Radiation therapy is often used alongside surgery or chemotherapy, but with the risk of damaging nearby healthy tissues.[13,18-20] Emerging therapies like photodynamic, photocatalytic, and sonodynamic therapy aim to enhance treatment precision and minimize side effects through spatiotemporal control over drug activation.[11,21]

1.4. Role of Chemotherapy in Cancer Treatment

Chemotherapy is a cornerstone of cancer treatment, playing a critical role in managing the disease across various stages and types.[12-15,22-24] It involves the use of chemical compounds to kill or inhibit the growth of cancer cells, often by causing DNA lesions, arresting DNA replication, activating several transduction pathways, which finally lead to necrosis or apoptosis, etc. These compounds are also known to induce cellular apoptosis through oxidative stress via the generation of ROS. Additionally, these drugs also lead to disruption of cell functioning by disrupting normal calcium homeostasis.[22,23,24] Chemotherapy can be used in different contexts, depending on the goals of treatment.[23,24] For example, neoadjuvant chemotherapy is administered before surgery to shrink tumors and make them easier to remove, while adjuvant chemotherapy is given after surgery to eliminate any remaining cancer cells and reduce the risk of recurrence.[25] In cases of advanced or metastatic cancer, palliative chemotherapy may be used to relieve symptoms, improve quality of life, and prolong survival.[26] . Many chemotherapeutic drugs target the

DNA of cancer cells, preventing them from replicating and ultimately leading to cell death.[22-24] Others disrupt the machinery involved in cell division, such as microtubules, or inhibit enzymes like topoisomerase that are essential for DNA replication.[22-24,27,28] Chemotherapy is often used in combination with other treatments, such as surgery, radiation therapy, and immunotherapy, to enhance its effectiveness and address the diverse nature of cancer.[29,30]

1.4.1. Organic Molecule-Based Chemotherapeutic Drugs

Chemotherapeutic drugs are classified into several categories (first generation, second generation, and third generation) based on their mechanism of action and chemical structure.[23,24] Each class of drugs damages cancer cells in a specific way, making them suitable for different types of cancer and treatment regimens.[22-24] Anthracyclines, including doxorubicin (Figure 1.4), intercalate into DNA, inhibiting the enzyme topoisomerase II, leading to DNA breaks and cell death.[31,32] Antimetabolites, like 5-fluorouracil and methotrexate (Figure 1.4), mimic the building blocks of DNA and RNA, disrupting their synthesis and halting cell growth.[33,34] Alkylating agents, such as cyclophosphamide (Figure 1.4), work by adding alkyl groups to DNA, causing damage that prevents the cancer cells from dividing.[34,35] These drugs can be administered either orally or intravenously, depending on the specific drug and the type of cancer being treated.[23,36] The pharmacokinetics of chemotherapeutic agents- how they are absorbed, distributed, metabolized, and excreted- play a crucial role in determining their efficacy and side effects.[23,24,37]

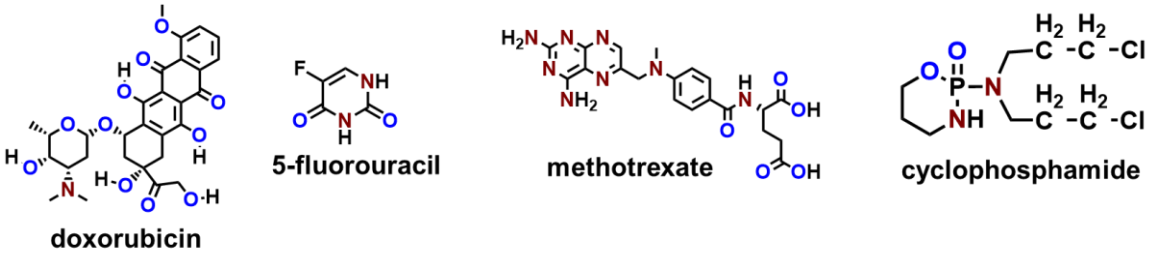

Figure 1.4: A few FDA-approved organic chemotherapeutic drugs.

1.4.2. Origin of Platinum-Based Chemotherapeutic Drugs

Before the 1960s, only organic compounds were used to treat cancer.[38,39] Rosenberg *et al.* in 1965 opened an avenue of previously unexplored transition metal-based chemotherapeutic drugs with cisplatin.[40] Since then, many transition metal complexes have been investigated for potential anti-cancer activity.[22-24] Cis-diamminedichloroplatinum(II), commonly known as cisplatin, is a potent anti-cancer agent due to its ability to treat a variety of cancers, including testicular, ovarian, head and neck, bladder, lung, cervical cancer, melanoma, lymphoma, etc.[12,22,23,24] Once cisplatin enters

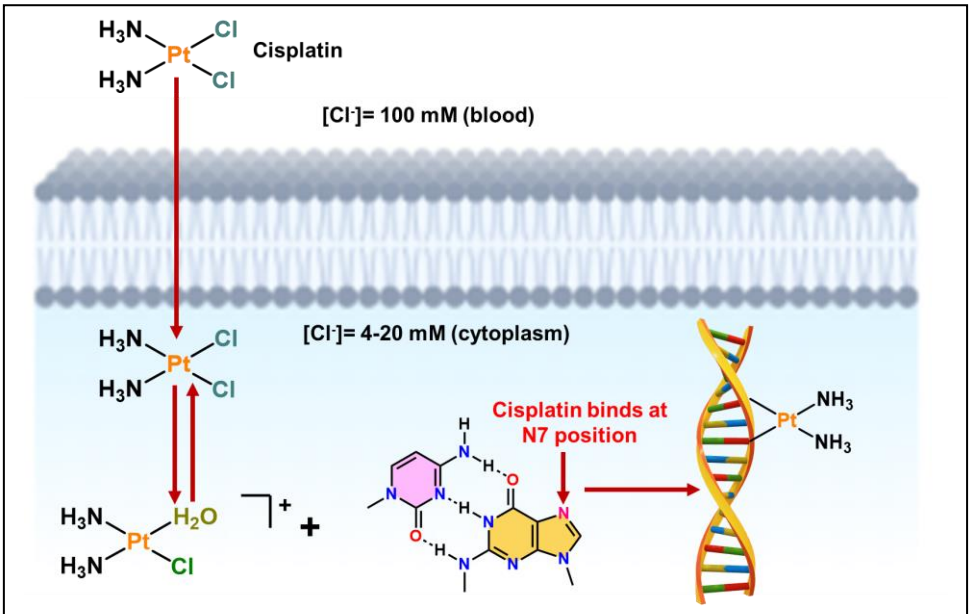

Figure 1.5: Pictorial representation of the mechanism of action of cisplatin.

the cells, one of the chloride ligands of cisplatin is replaced by water molecules or sulfhydryl groups present in the cytoplasm, after which it becomes highly electrophilic (Figure 1.5).[22-24] Therefore, it binds easily with the N7 position of the purine base, guanine, present in the DNA via intra-strand crosslinks formation (Figure 1.5).[12,22-24] Once it binds with DNA, it leads to DNA lesions, arresting DNA replication, activating several transduction pathways, which finally lead to necrosis or apoptosis.[12,22-24] Despite having therapeutic success over certain cancers, it induces various toxic side effects like nephrotoxicity, neurotoxicity, hepatotoxicity, and ototoxicity.[12,14,15,23,24,42] Also, the long-term use of cisplatin has undesirable effects on normal tissues.[12,14,15,23,24] The resistance, such as intrinsic resistance and acquired resistance, is either present in the body or develops during persistent treatment.[23,41] Cisplatin's chloride ligand is extremely labile, which increases the reactivity of the compound and is hence mainly responsible for toxicity due to cisplatin.[22-24] To overcome these problems, other Pt-based drugs were investigated for their anti-cancer activity. Some examples include carboplatin, oxaliplatin, lobaplatin, nedaplatin, and heptaplatin (Figure 1.6).[22-24,37,38,42] Compared to cisplatin, carboplatin unveils a lower aquation rate due to the presence of a bidentate ligand, which is comparatively less labile than chloride and therefore has reduced toxicity.[23,24,43] Carboplatin can be used for aggressive tumors, as these tumors require high dosages, and it can be used long-term with low toxicity.[23,24,43] However, despite these advantages over cisplatin, carboplatin also faces the drug resistance issue, which eventually develops during the treatment.[23,24,38] Therefore, oxaliplatin was developed to overcome this.[23,24,38] Unlike cis-platin, oxaliplatin contains dicarboxylate as the leaving group and 1,2 diamminocyclohexane as the carrier ligand.[22-24,43] The presence of 1,2-

diamminocyclohexane as the carrier ligand enhances the lipophilicity, which further helps to overcome the drug resistance issue of cis-platin by enhancing the cellular uptake of oxaliplatin inside the cancerous cell.[22-24,43] Oxaliplatin has a similar mode of action to that of cisplatin.[22-24,43] It also disrupts DNA replication and transcription by creating intrastrand linkages between two guanine residues or a guanine and an adenine, but it does not produce cross-resistance like cisplatin or carboplatin.[23,24,38,43] As a result, oxaliplatin and cisplatin have a complementary impact on anticancer treatment and have been widely utilized.[23,24,38,43]

In continuation of efforts to enhance efficacy, reduce systemic toxicity, and overcome drug resistance, third-generation platinum-based drugs such as lobaplatin, nedaplatin, and heptaplatin were introduced.[22-24,42] Lobaplatin, containing a 1,2-diaminocyclobutane ligand and a lactate leaving group, exhibits higher water solubility, stability.[22-24,42,43] It shows antitumor activity with reduced nephrotoxicity and neurotoxicity.[22-24,42,43] It also exhibits activity against cisplatin-resistant cells.[22-24,42,43] Lobaplatin is approved in China for treating small-cell lung cancer, breast cancer, and chronic myelogenous leukemia.[22-24,42] Nedaplatin with a glycolate ligand offers similar DNA cross-linking activity.[22-24,42,43] It is reported to show significantly reduced nephrotoxicity, making it more suitable for patients with renal impairment. It is approved in Japan for head and neck, esophageal, and non-small-cell lung cancers.[22-24,42] Heptaplatin with a malonic acid moiety and alicyclic amine ligand retains cisplatin-like DNA binding properties.[22-24,42,43] Interestingly, it shows increased activity in resistant gastric cancers while demonstrating lower gastrointestinal and renal toxicity. Heptaplatin got approval in South Korea for gastric cancer treatment.[22-24,42]

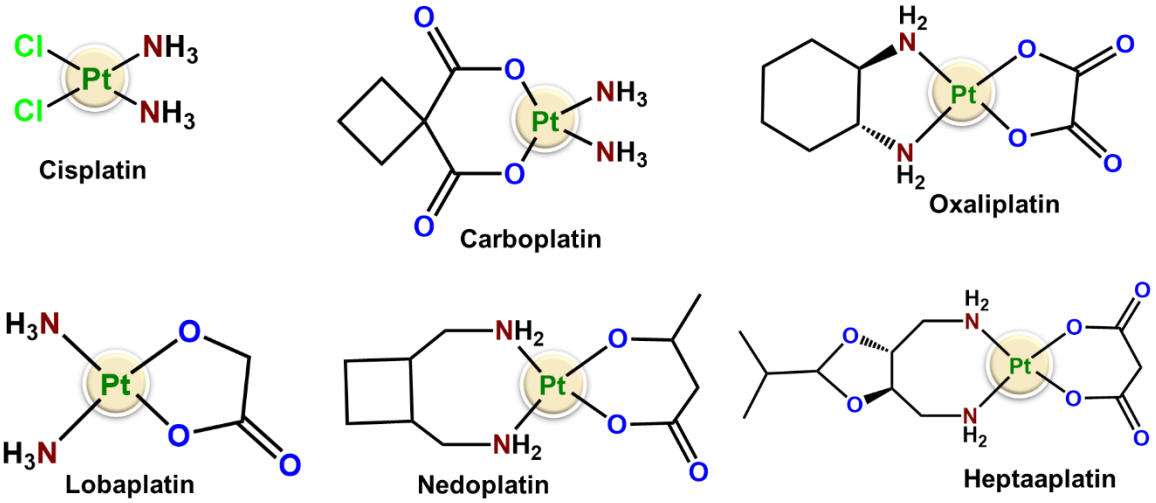

Figure 1.6: Structures of some Pt(II) based chemotherapeutic agents.

1.4.3. Drawbacks and Side Effects of Chemotherapy

While chemotherapy has revolutionized cancer treatment, it is associated with significant drawbacks and side effects that can impact patients' quality of life.[12,14,15,22-24] One of the most common side effects is myelosuppression, a reduction in the production of blood cells by the bone marrow, which can lead to anemia, increased risk of infections, and bleeding disorders.[44] Chemotherapy also frequently causes nausea and vomiting, which can be severe and debilitating.[14,15,22-24,45] Hair loss, or alopecia, is another well-known side effect, as chemotherapy targets rapidly dividing cells, including those in hair follicles.[46] Another major limitation of chemotherapy, particularly with platinum-based drugs, is the development of drug resistance upon administration of repeated doses, which reduces the efficiency of the drugs.[12,14,15,22-24] This resistance arises partly due to the inactivation of platinum drugs by intracellular thiol-containing species such as glutathione and metallothioneins.[23,24,47] The nucleotide excision repair (NER) mechanism also contributes

to drug resistance by repairing the DNA-cisplatin adduct.[22-24,48] Platination of DNA results in DNA kinking, which is an unusual change in DNA conformation that is recognized by NER proteins (Figure 1.7), leading to the excision of the DNA strand.[22-24,48] In the next step, DNA polymerase acts on the excision site to repair the DNA (Figure 1.7), which results in the inactivation of cisplatin for cancer treatment (Figure 1.7).[22-24,48] In addition to these acute side effects and drug resistance, chemotherapy can cause long-term complications, such as organ damage.[14,15,22-24] For example, anthracyclines (like doxorubicin) are known to cause cardiotoxicity, which can lead to heart failure.[14,15,22-24] Chemotherapy can also increase the risk of developing secondary cancers later in life due to its DNA-damaging effects.[14,15,22-24]

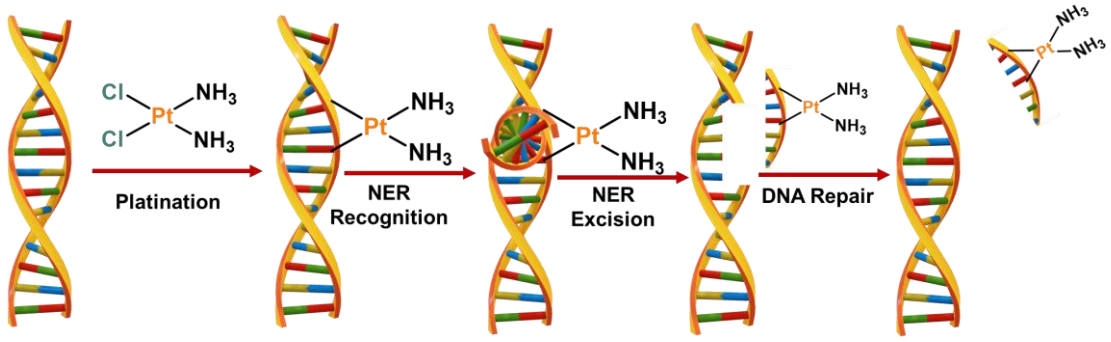

Figure 1.7: Scheme of the steps involved in the NER mechanism.

1.4.4. Strategy to Overcome the Drawbacks of Chemotherapy

Chemotherapy remains a cornerstone of cancer treatment, but is often hindered by significant limitations such as non-selective cytotoxicity, severe systemic side effects, multidrug resistance (MDR), and low tumor specificity. These factors collectively reduce its therapeutic efficacy.[12,14,15,22-24,48] To address these drawbacks, several innovative

strategies have emerged, e.g., (i) targeted drug delivery systems: including attachment of tumor targeting moiety or antibody-drug conjugates to deliver chemotherapeutic agents specifically to tumor tissues while minimizing damage to healthy cells;[49,50] (ii) prodrug approaches: involve selective activation of prodrug by intracellular reduction or photosubstitution in the tumor microenvironment; [51,52] (iii) stimuli-responsive drug activation: involves the selective activation of the drug at the target site by external stimuli such as light (photodynamic therapy and photocatalytic therapy), or ultrasound (sonodynamic therapy), which offers spatiotemporal control over drug activation that can reduces off-target toxicity and minimize damage to healthy cells;[11,20] (iv) the combination therapies integrating chemotherapy with immunotherapy, radiotherapy, or targeted agents have shown synergistic effects and can overcome resistance mechanisms by damaging cancer cells through multiple pathways.[53-55]

1.5. Photodynamic Therapy

Photodynamic therapy (PDT) has attracted considerable interest as an alternative cancer treatment due to its various advantages over traditional cancer therapy, such as (i) it selectively targets and destroys tumor cells while preserving healthy cells;[56-63] (ii) it is noninvasive;[56-63] (iii) highly selective, and [56-63] (iv) additionally, it promotes faster healing with little to no scarring.[56-63]

The steps involved in PDT are given in Figure 1.8[64-66]

- The first stage is the introduction of the photosensitizer (PS) into the body.

• In the second stage, the photosensitizer accumulates around the tumor tissue during a period of incubation.

• The third stage involves irradiation of the tumor tissue with a suitable wavelength of light, which excites the photosensitizer and generates cytotoxic reactive oxygen species (ROS).

• Finally, in the fourth stage, these ROS react with biological substrates such as nucleotides, amino acids, proteins, and lipids, disturbing normal cell functions and inducing cell death.

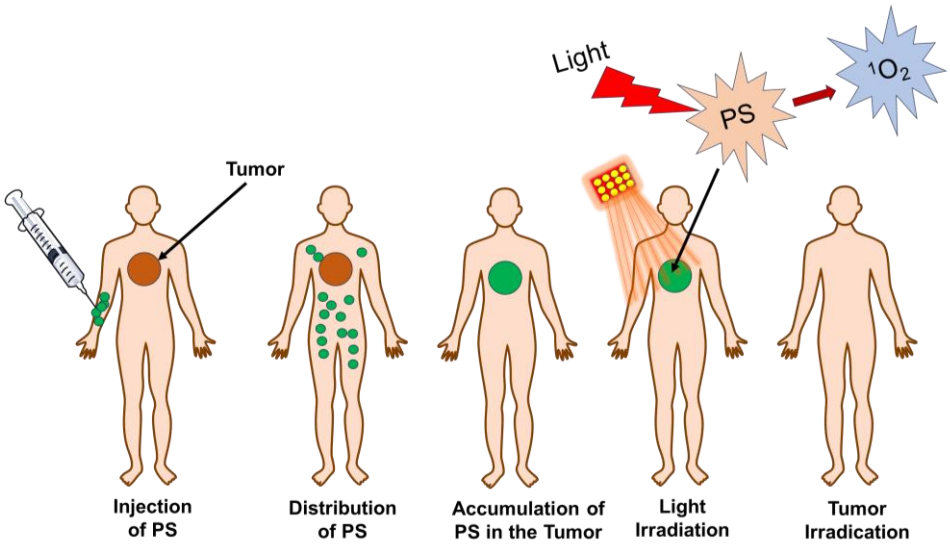

Figure 1.8: Schematic representation of different stages of PDT.

1.5.1. Mechanism of Action

Light absorption causes the photosensitizer to move from a singlet ground state (S_0) to a triplet excited state (generally T_1) via a singlet excited state.[67-69] In T_1 excited state, photosensitizer have two possibility, either it transfer electron to biomolecule (*via* type I reaction) and that biomolecule further react with tissue oxygen to generate free radicals

such as $^{\cdot}OH$, $O_2^{\cdot-}$, and H_2O_2 or they can transfer energy directly to molecular oxygen (*via* type II reaction) and transform it into highly reactive singlet oxygen species (Figure 1.9).[67-69] These generated ROS causes protein damage, lipid oxidation, DNA damage, and finally destruction of cancer cells.[67-69]

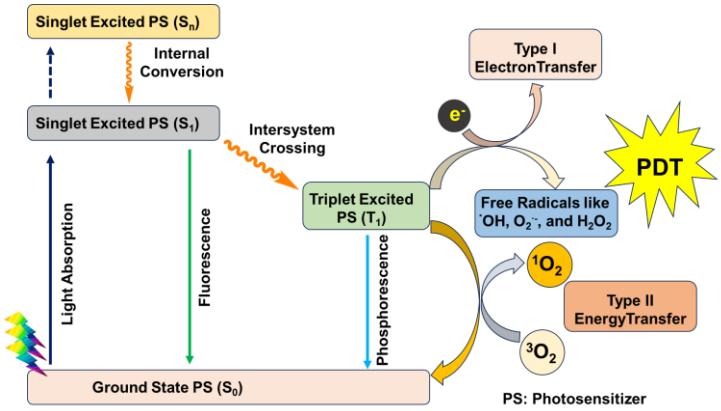

Figure 1.9: Schematic representation of type I/II PDT.

1.5.2. Organic Photosensitizers

Currently, a few organic compounds, mostly porphyrin derivatives such as photofrin, Visudyne, Foscan, etc. (Figure 1.10), have been approved for clinical use as PDT drugs.[70-72] The FDA-approved, most extensively researched, and widely used PDT drug is photofrin, which has been used for the treatment of early- and late-stage lung cancers, esophageal cancer, bladder cancer, and early-stage cervical cancer in countries including Canada, Japan, the United States, and various European nations.[59,60,73,74] Although photofrin is widely used for Esophageal, lung, and bladder cancer, cervical cancer treatment, it still poses a number of limitations, e.g., (i) skin sensitivity as it also localizes in skin tissues;[74,75] (ii) hepatotoxicity as the metabolized product of photofrin is bilirubin.[74,75] Additionally, porphyrins and organic photosensitizers suffer from poor

solubility and photostability (prone to degradation with prolonged light exposure).[59,74,75]

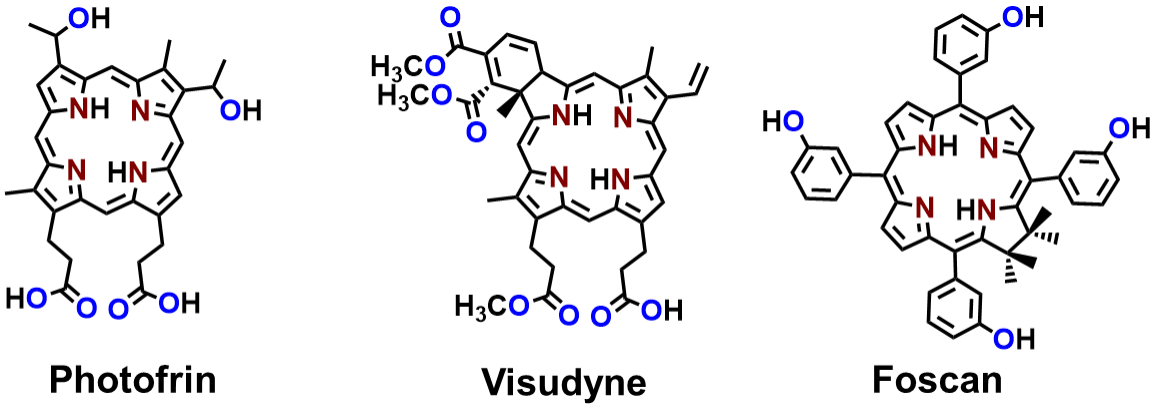

Figure 1.10: Structures of some organic photosensitizers for PDT.

1.5.3. Photosensitizers based on Transition Metal Complexes

The limitations associated with organic and porphyrin-based photosensitizers have driven significant interest in the development of transition metal-based alternatives.[56-63] These metal-based photosensitizers offer distinct advantages, primarily due to their high degree of structural tunability.[56-58] By modifying the coordinated ligands, it is possible to precisely control critical properties such as solubility, stability, and target specificity.[77-79] Furthermore, the ligand environment can be engineered to shift the absorption profile toward longer wavelengths, such as red or near-infrared light, which penetrate tissues more effectively.[77-79]

Heavy metal-containing complexes (such as Ru, Ir, Pt, Os, etc.) generally tend to exhibit longer-lived excited states, facilitating efficient energy transfer and higher ROS quantum yields under PDT conditions.[80-83] While organic photosensitizers have their own merits, metal complexes often outperform them in applications where photostability, prolonged excited-state lifetimes, and precise delivery to target tissues are essential.[80-83] A broad

range of transition metal complexes, including those based on ruthenium (Ru), iridium (Ir), osmium (Os), platinum (Pt), and palladium (Pd), have been investigated for PDT applications.[56-63] Among these, palladium and ruthenium-based complexes, such as WST09 (padoporfin), WST11, and TLD-1433, have progressed into clinical trials, demonstrating the promising therapeutic potential of transition metal-based complexes (Figure 1.11).[74-76,84] TLD1433, a Ru(II)-based photosensitizer for the treatment of non-muscle invasive bladder cancer, enters clinical trial.[75,76] These transition metal compounds underscore the growing recognition of transition metal complexes as next-generation photosensitizers, offering multifunctional capabilities, enhanced phototoxic effects, and the potential for precision-targeted cancer therapy.[55-62,74-76]

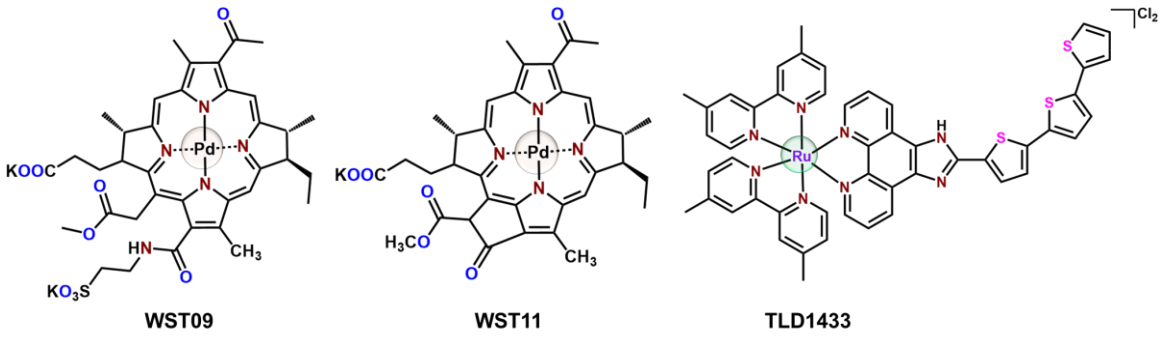

Figure 1.11: Structures of metal-based photosensitizers that were/are in clinical trials.

1.5.4. Drawbacks of Photodynamic Therapy

Even though PDT has emerged as a promising alternative to conventional cancer treatments, it is associated with a few limitations that hinder its widespread clinical application.[85-87] One of the major drawbacks of PDT is its complete dependency on molecular oxygen for the generation of reactive oxygen species (ROS), making it less

effective in the hypoxic microenvironments commonly found in solid tumors.[85-87] The second major drawback of PDT is that it is effective against only specific types of cancers, like skin, esophageal, or lung cancer, and not for all cancer types.[85-87]

These limitation highlights the necessity of developing novel strategies, such as oxygen-independent photosensitizers, and combination therapies, to enhance PDT's therapeutic potential.[11]

1.6. Photocatalytic Cancer Therapy

In response to these challenges, photocatalytic cancer therapy (PCT) has emerged as a promising next-generation cancer treatment modality.[11] Although this therapy is traditionally characterized by its dual-mode ROS generation *via* type I/II pathways, the true therapeutic potential of PCT lies in its ability to disrupt cancer metabolism through the photoinduced oxidation of nicotinamide adenine dinucleotide (NADH).[11] Unlike PDT, which suffers from oxygen dependency, PCT leverages NADH oxidation as a robust oxygen-independent mechanism to overcome hypoxia-associated resistance.[11] NADH plays an important role in cellular redox balance and serves as a key electron donor in the mitochondrial electron transport chain.[85,86] Its oxidation not only deprives cancer cells of metabolic energy but also contributes to redox imbalance, triggering cell death.[87-89] This metabolic disruption through NADH photo-oxidation represents a central therapeutic mechanism of PCT, with ROS generation acting synergistically to amplify oxidative stress within cancer cells.[11] The metabolic disruption through NADH oxidation provides a novel mechanism of action to this therapy that may help to overcome the PDT-based drug resistance problem.[11]

1.6.1. Transition Metal-based Photocatalysts in Photocatalytic Cancer Therapy

Transition metal-based photocatalysts, especially Ir(III), Ru(II), and Os(II) complexes, are explored for this approach because of their favorable photophysical properties like high photostability, strong spin-orbit coupling, and tunable absorption in the visible region (Figure 1.12).[11,93-108] Several studies, including those from the groups of Sadler, Huang, Ruiz, Paira, as well as our group, have demonstrated that photocatalysts based on these metals induce photocytotoxicity through a combination of NADH oxidation and ROS generation.[93-108] Among these, the oxidation of NADH has emerged as a crucial determinant of therapeutic efficacy, particularly under oxygen-deprived conditions.[93-108]

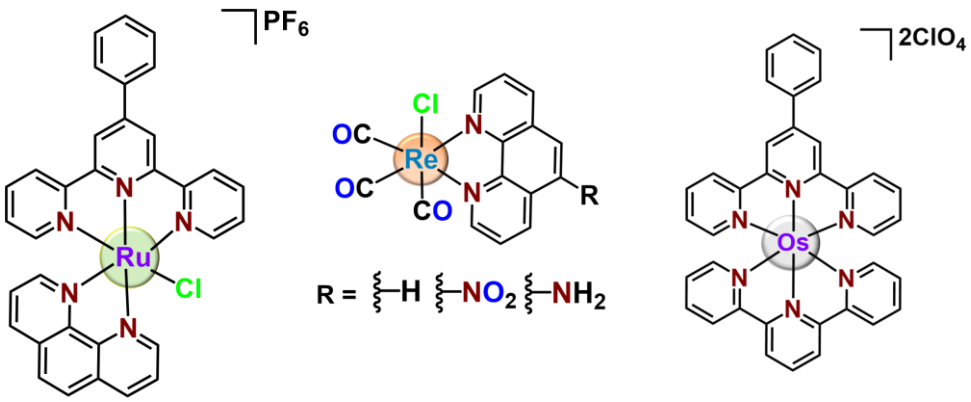

Figure 1.12: Structures of a few previously reported photocatalysts.

1.6.2 Ir(III)-based Photocatalysts

The first in-cell catalytic photo-oxidation of NADH with Ir(III)-photocatalyst *viz*., [Ir(ttpy)(pq)Cl]PF_6 (**Ir1**) (Scheme 1.1) was reported by Sadler *et al.*[93] **Ir1** displayed high excited state lifetime in acetonitrile (743.7 ns in air and 1390.3 ns in N_2) or PBS (330.8 ns in air and 382.3 ns in N_2) and favorable redox behavior (high excited-state reduction

potential ($E_{1/2}^{*III/II}$ = +1.22V) than $E_{NAD^+/NADH}$ = +0.32 V), which were crucial for NADH oxidation photocatalysis.[93] The DFT calculations also revealed a 'clamped' formation between π–π adducts of excited-state **Ir1*** and NADH to facilitate electron transfer in the presence of light. Therefore, **Ir1** successfully oxidized NADH to NAD^+ with a turnover number (TON = 50.2) and turnover frequency (TOF = 100.4 h^{-1}) upon the blue light (465 nm, 8.9 J/cm^2) exposure.[93]

Mechanistically, NADH photo-oxidation occurred *via* the following steps: (i) Light activation of **Ir1** to a triplet state (via a singlet state) **Ir1***.[93] (ii) **Ir1*** was highly oxidative and extracted an electron from NADH, forming a highly reducing **Ir1**$^{-\bullet}$ species and $NADH^{+\bullet}$ radical (Scheme 1.1a). $NADH^{+\bullet}$ were then converted to $NAD^{\bullet}$ radicals, confirmed by the EPR studies with CYPMPO as the spin trap. (iii) Under normoxia, **Ir1**$^{-\bullet}$ reacted with molecular oxygen via an electron transfer pathway to form $O_2^{-\bullet}$ radicals and regenerate the **Ir1** (Scheme 1.1a). (iv) $O_2^{-\bullet}$ then accepted one electron from $NAD^{\bullet}$, producing NAD^+ and H_2O_2 (confirmed by the H_2O_2 detection strip).[93] One of the major issues in cancer drug development research is delivering hypoxia-active drug molecules.[93] Interestingly, **Ir1** was also active in hypoxia for NADH oxidation. As shown in Scheme 1.1b, under hypoxia,

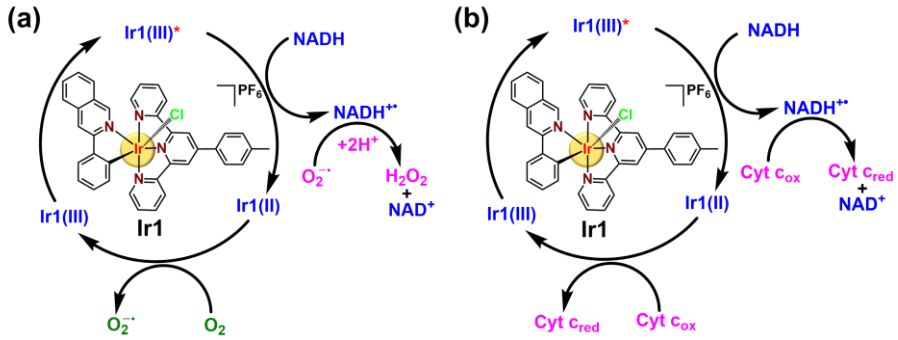

Scheme 1.1: NADH oxidation photocatalytic cycle for **Ir1**, **(a)** under normoxia, and **(b)** under hypoxia.

Fe^{3+}–cytochrome c (Fe^{3+}–cyt c) could serve as the electron acceptor instead of molecular O_2.[93] This pathway provides oxygen-independent NADH photo-oxidation, useful for photo-redox catalysis under a hypoxic environment. Besides NADH photo-oxidation, **Ir1** in the triplet state also interacted with O_2 via a type II energy transfer pathway and generated $^1O_2$. In A549 (human lung carcinoma) cells, **Ir1** was located within the mitochondria, the cellular organelle with high NADH concentration (10^{-6}-10^{-3} M).[93] **Ir1** also oxidized NADH in A549 cells (Figure 1.13a) after 465 nm light exposure, which in turn generated H_2O_2 in A549 cells (Figure 1.13b) under normoxic conditions. As NADH is involved in the ATP generation process, the oxidation of NADH led to the depletion of ATP in A549 cells (Figure 1.13c).[93] **Ir1** showed phototoxicity against A549, NCI-H460 (lung), HeLa (cervix), HepG2 (liver), and SGC-7901 (gastric) cancer cells in normoxia (IC_{50} *ca.* 1.0-1.9 μM) and hypoxia (IC_{50} *ca.* 2.3-8.7 μM), while had low toxicity in the dark (IC_{50} = 31-42 μM) towards normal LO2 (human hepatocyte) and MRC-5 (human lung fibroblasts) cells.

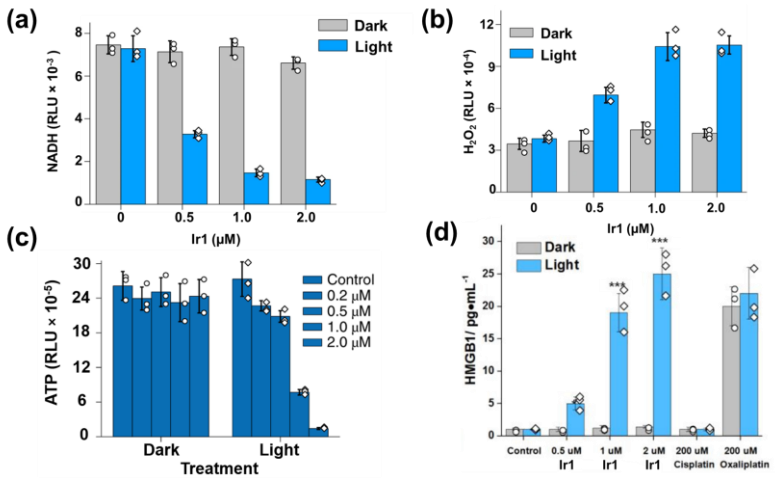

Figure 1.13: Concentration of (a) NADH, (b) H_2O_2, and (c) ATP in A549 cells exposed to **Ir1** under light (465 nm, 8.9 J/cm^2) or dark. (d) Increase in HMGB1 concentration after **Ir1**+Light treatment, indicating immunogenic cell death. Reproduced from ref 90.

Under 465 nm (8.9 J/cm^2) light, **Ir1** caused a significant decrease in the mitochondrial membrane potential (MMP) due to NADH depletion, and ETC disruption under normoxic and hypoxic conditions.[93] This photocatalyst induced immunogenic apoptosis was confirmed with HMGB1 enzyme-linked immunosorbent and Calreticulin immunofluorescence assays (Figure 1.13d). It is important to note that during immunogenic apoptosis, the drug eliminates cancerous cells while simultaneously stimulating the immune response.[93] This dual action ensures long-lasting therapeutic effects, reduces the risk of cancer recurrence, and addresses challenges posed by therapy resistance.[90] Overall, this work, for the first time, indicated the potential of Ir(III) photocatalyst in PCT under blue light irradiation through two different pathways under normoxia and hypoxia, and kill cancer cells by immunogenic apoptosis.

Ruiz *et al.* highlighted the photocatalytic efficiency of dppz and benzimidazole-appended Ir(III) photocatalysts **(Ir2-Ir5,** Figure 1.14**)** in NADH photo-oxidation.[94] The functionalized benzimidazoles were designed to enhance the lipophilicity of the photocatalysts.[94,110] The p-trifluoromethyl benzyl groups and chromophoric 2-(5-arylthiophen-2-yl)benzothiazoles were used to red-shift the light absorption.[94] These photocatalysts oxidized NADH in PBS:DMF (95:5, v/v) under blue (465 nm, 0.5 mW/cm^2) and green (520 nm, 2.0 mW/cm^2) light. **Ir5** achieved the highest TOF of 403.1 h^{-1} under 465 nm light. However, under 520 nm light, the TOF was reduced significantly to 38.9 h^{-1} for **Ir5**. The introduction of the electron-donating N,N-dimethylaminophenyl substituent in **Ir5** significantly improved its NADH photo-oxidation ability compared to other Ir(III) photocatalysts containing only trifluoromethyl groups.[94] Under 405 nm laser irradiation, the lysosome-localizing **Ir5** induced ROS-mediated lysosomal membrane damage, causing

the release of acidic lysosomal contents into the cytoplasm, triggering oncotic-like cell death, a distinct and often underutilized cell death pathway in PDT.[94,110] Although the anticancer effect of **Ir2-Ir5** was quite promising in 2D cell cultures, their efficacy drastically diminished in 3D cell models. They suggested that the high lipophilicity and self-aggregation of **Ir2-Ir5** hindered their penetration into the layers of the 3D spheroids, thereby reducing their effectiveness in reaching the hypoxic core of the spheroids.[94]

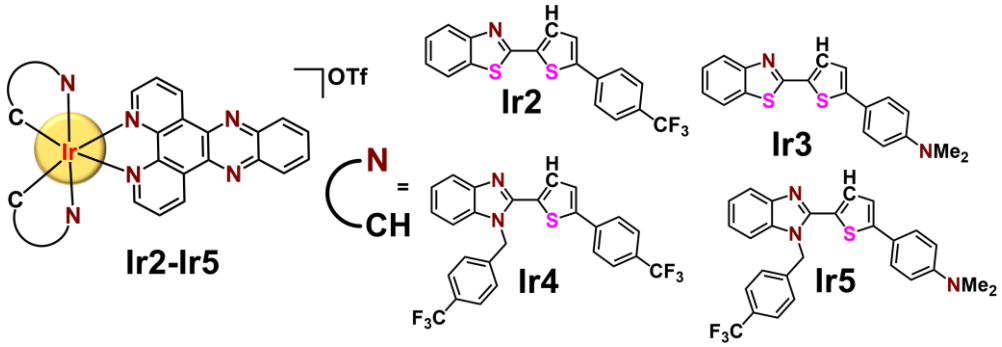

Figure 1.14: Structures of **Ir2-Ir5**.

Huang *et al.* and our group reported a novel mononuclear Ir(III) photocatalyst (**Ir6)** along with its dinuclear analogue (**Ir7**) (Figure 1.15a).[95] The incorporation of an additional Ir(III)-center in **Ir7** significantly improved the excited-state reduction potential (+1.42 V *vs*. Ag/AgCl) and excited-state lifetime (τ = 3.62 µs in N_2 saturated CH_2Cl_2). Henceforth, the photocatalytic NAD(P)H oxidation efficacy of **Ir7** (TOF = 437.1 h^{-1}) was found to be *ca.* 13 times higher than **Ir6** (TOF = 36.2 h^{-1}) under 525 nm exposure, revealing the synergistic effect of the additional Ir(III) center and discarding the additive effect.[95] A similar trend was also reflected in their phototoxicities, where **Ir7** displayed much higher toxicity against HepG2 cells (IC_{50} = 0.3 µM) than **Ir6** (IC_{50} = 15.7 µM) with a photo-therapeutic index (PI) > 666.7 (PI = Dark IC_{50}/Light IC_{50}) under normoxic conditions after

525 nm (29.56 J/cm^2) light irradiation. **Ir7** showed reduced phototoxic activity (IC_{50} = 25.7 μM) under hypoxia conditions. SC-ICP-MS (Single-cell inductively coupled plasma mass spectrometry) was used to quantify the Ir uptake and retention within individual cells (Figure 1.15b). **Ir7** showed more than two times higher Ir content per single cell than **Ir6**, correlated with the high lipophilicity of **Ir7** (log P **Ir6**/**Ir7**, 0.13/0.54). The in-cell amount of **Ir7** ranged from 20-400 ag per cell with time progress (4-12 h), indicating its high retention within HePG2 cells. **Ir7** was also *in vivo* biocompatible in the zebrafish model (Figure 1.15c) and mouse models. **Ir7** also presented an encouraging photo-cytotoxic profile against the HepG2 cell tumor-bearing mice (Figure 1.15d). Tumor growth was reduced after **Ir7**+Light treatment (Figure 1.15d) compared to the control, light-only, and **Ir7**-only groups.[95]

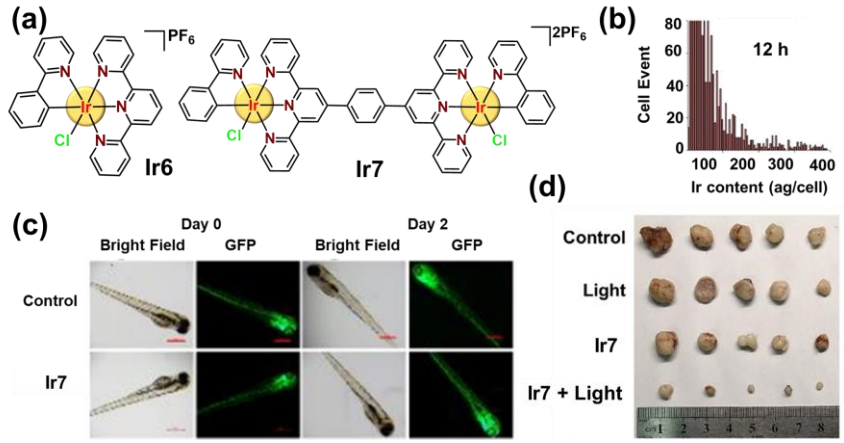

Figure 1.15: (a) Structures of **Ir6** and **Ir7**. (b) SC-ICP-MS histograms showing the Ir-uptake in **Ir7** (10 µM)-treated HepG2 cells. (c) The bright green fluorescence of GFP after 48 hours of incubation with **Ir7** in the FLK strain of zebrafish demonstrates **Ir7**'s biocompatibility. Scale bar: 500 µm. (d) Images of tumors from mice bearing HepG2 cells under various treatment conditions, highlighting the *in vivo* effectiveness of **Ir7** under light (525 nm, 88.68 J cm^{-2}). Reproduced from ref 95.

Recently, Singh et al. demonstrated the photocatalytic NADH oxidation efficiency of another Ir(III)-based dinuclear complex, **Ir8** (Figure 1.16) (TON = 26.3, TOF = 10.52 min^{-1}). [96] The rate of NADH oxidation was only slightly affected in the presence of NaN_3 ($^1O_2$ scavenger), indicating **Ir8** can oxidize NADH even in the presence of $^1O_2$.[96] **Ir8** was active against MCF-7, CT26 (colorectal cancer), and PT45 (pancreatic ductal adenocarcinoma) cancerous cells under 465 nm light (IC_{50} ca. 3-10 μM).[96] In a significant advancement, Sadler *et al*. developed a heterodinuclear complex, **Ir9** (Figure 1.16), which combined photoactivated chemotherapy (PACT) and PCT to achieve synergistic anticancer effects.[96] Upon 465 nm, 4.8 mW cm^{-2} light exposure, **Ir9** oxidized NADH, contributing to its therapeutic action.[96] **Ir9** exhibited photocytotoxicity (IC_{50} 1.3-9.7 μM) within 60 min of light irradiation against A2780 (ovarian), A549, and PC3 (prostate) cancer cells.

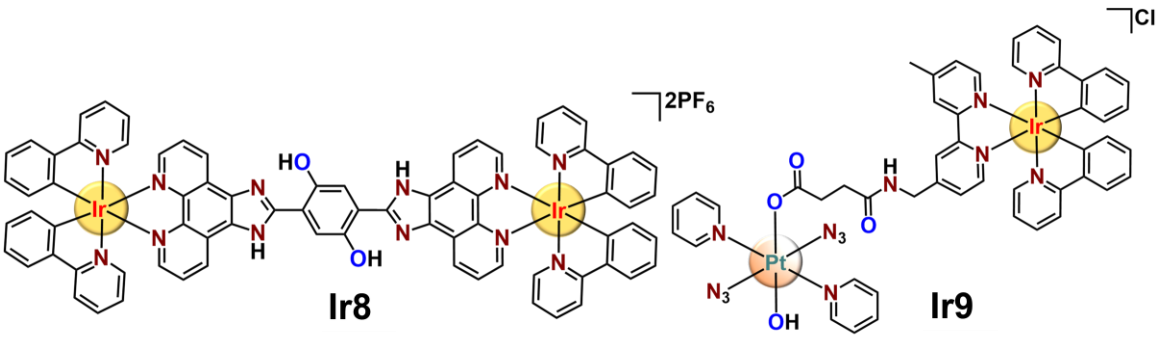

Figure 1.16: Structures of **Ir8** and **Ir9**.

Gou *et al.* reported a naphthalene diimide appended Ir(III) photocatalyst, **Ir10** (Figure 1.17), decorated with a strong electron acceptor and excellent charge carrier moiety (Figure 1.17).[97] The NDI moiety attached in **Ir10** shifted the absorption band to ~635 nm. The TOF value of **Ir10** for NADH photo-oxidation was 270.6 h^{-1} at 635 nm light. **Ir10** showed light-mediated NADH oxidation and ATP depletion inside the 4T1 cancer cells. Further,

the photocytotoxicity study revealed that **Ir10** showed potent 635 nm light-triggered photocytotoxicity under normoxic and hypoxic conditions (1% O_2) against 4T1 cells.[97] In addition to apoptotic cell death, **Ir10** displayed GPX4-catalyzed detoxification of lipid peroxidation due to decreased GSH concentration, indicating the occurrence of ferroptosis. Moreover, the *in vivo* investigations demonstrated *ca*. 89% tumor growth inhibition rate in the Balb/c mice model.[97]

Paira *et al.* reported a PTA (1,3,5-triaza-7-phosphaadamantane) containing half-sandwich anticancer Ir(III) complex, **Ir11** (Figure 1.17).[98] PTA complexes are known to have extraordinary thermodynamic and GSH stability.[98] The absorption band of **Ir11** ranged from the UV to the blue region. Therefore, it produced a significantly lower TOF (0.201 h^{-1}) for NADH oxidation upon visible light exposure (400-700 nm). However, **Ir11** exhibited good photocytotoxicity against triple-negative breast cancer cells (IC_{50} = 2.80 µM), which was correlated with its superior DNA intercalation capability.[98]

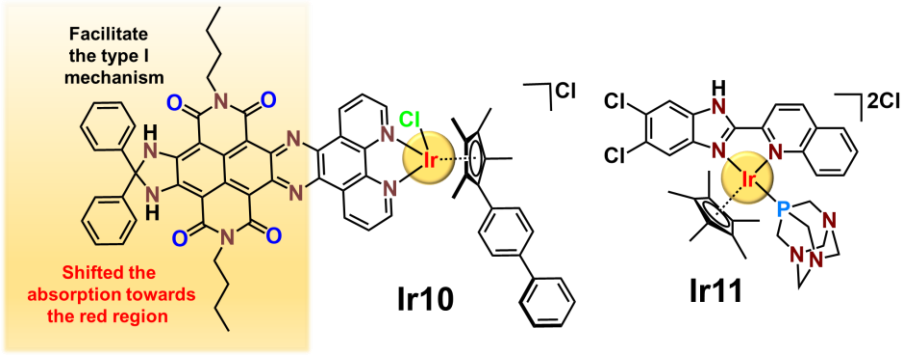

Figure 1.17: Structures of **Ir10** and **Ir11.**

The 2-phenyl pyridine and coumarin 6 appended Ir(III) photocatalysts, **Ir12-Ir14** (Figure 1.18a),[99] which oxidized NAD(P)H *via* a different mechanism, have been reported recently by Huang *et al*. Upon light exposure, (i) **Ir14** moved to its excited state **Ir14***. (ii) At the excited-state, **Ir14*** transferred an electron to O_2 to form $O_2^{-\bullet}$ (dihydroethidium probe

confirmed $O_2^{-\bullet}$ formation in cells) and a highly oxidizing **Ir14(IV)** species. (iii) the highly oxidizing **Ir14(IV)** then extracted an electron from NAD(P)H, regenerating **Ir14** and producing $NAD(P)H^{+\bullet}$ (EPR study confirmed $NAD(P)H^{+\bullet}$ formation) (Figure 1.18b).[99] ^1H NMR studies indicated complete oxidation of NAD(P)H to $NAD(P)^+$. NAD(P)H oxidation efficiency of **Ir14** reduced significantly under N_2, indicating the crucial role of O_2 in photocatalysis.[99] The NAD(P)H oxidation TOF for **Ir14** was *ca*. 308 h^{-1} under 465 nm light (11.7 J cm^{-2}). This result was consistent in both aqueous medium and cancer cells. **Ir12** and **Ir13** also followed the same mechanism for NAD(P)H and NADH oxidation. **Ir14** selectively localized in mitochondria due to its high positive charge and changed the MMP, ultimately showing necro-apoptosis in 465 nm light-exposed human nasopharyngeal carcinoma (CNE-2Z) cells.[99] The *in vitro* experiments showed that **Ir14** was non-toxic to various normal cells in the dark and showed attractive phototoxicity

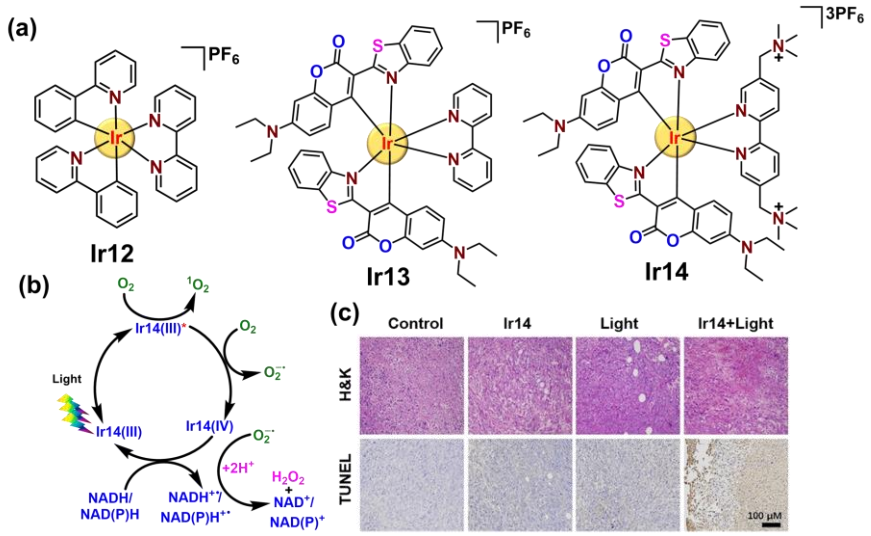

Figure 1.18: (a) Structures of **Ir12-Ir14**. (b) Catalytic cycle for NADH/NAD(P)H photooxidation by **Ir14** under normoxia. (c) H&E staining and TUNEL assay images of colon tumor tissues from mice under different treatments show that the **Ir14**+Light induces apoptosis. Reproduced from ref 99.

toward various cancer cells. Interestingly, even against cis-platin-resistant A549R cells, **Ir14** produced a promising anticancer effect (IC_{50} ~ 1.6 μM (under 465 nm light), *ca.* 50 times more active than *cis*-platin under identical experimental conditions. **Ir14**'s biocompatibility and non-toxic profile in the dark was confirmed using zebrafish models, where no tissue damage was observed in wild-type strain (AB strain) and transfected strain (FLK strain) embryos. In a CT26 colon carcinoma mouse model, **Ir14** showed no systemic toxicity without irradiation. In contrast, **Ir14**+Light (465 nm, 11.7 J cm^{-2}) inhibited tumor growth, confirming its excellent biocompatibility and potent photocatalytic anticancer activity *in vivo*. The H&E and tunnel study showed increased apoptosis and necrosis under **Ir14**+Light combination (Figures 1.18c). This underscores the potential of complex **Ir14** as an effective *in vivo* PCT agent.[99]

A crucial structure-activity relationship for NAD(P)H/NADH photo-oxidation was established, with **Ir15-Ir17** having differently substituted terpyridine and coumarin 6 ligands (Figure 1.19a).[100] **Ir15-Ir17** oxidized NAD(P)H/NADH *via* Figure 1.18b, where their T_1 state mainly acted as reductants. For example, in the excited state, **Ir17**

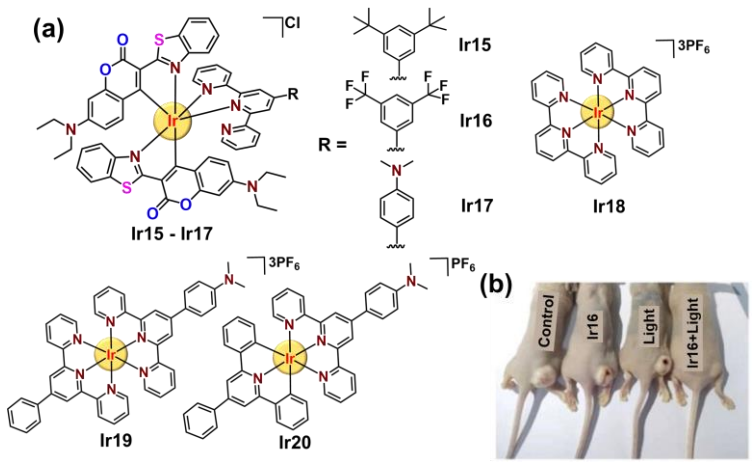

Figure 1.19: (a) Structures of **Ir15-Ir20**. (b) Images showing that the **Ir16**+Light significantly inhibited the growth of A431 tumor in mice after 14 days. Light dose: 465 nm, 11.7 J/cm^2. Reproduced from ref 100.

($[Ir^*]^+/[Ir]^0$) = +0.24 V, TOF = 1357.2 h^{-1}) is significantly more reductive than **Ir15** (+0.35 V, TOF = 1097.8 h^{-1}) and **Ir16** (+0.54 V, TOF = 1060.4 h^{-1}) indicating that the electron-donating NMe_2 group improved the electron donation ability of the catalyst which upon light activation donated electron to O_2.[100] Mitochondria localized **Ir16** showed nanomolar IC_{50} against HeLa cells with high PI values under 465 nm or 525 nm light exposure. *In vivo* studies with **Ir16** in A431 (epidermoid carcinoma) tumor-bearing mice *via* intra-tumor injection revealed that the **Ir16**+Light significantly reduced tumor size (Figure 1.19b).[100] Further, the H&E and tunnel study showed increased apoptosis and necrosis compared to controls, **Ir16** alone or light alone.[100]

In a subsequent study, three terpyridine-Ir(III)-photocatalysts (**Ir18-Ir20**, Figure 1.19a) are reported for NADH oxidation, where the dimethylamine auxochrome in **Ir19** and **Ir20** shifted the absorption maximum toward longer wavelengths.[101] Among **Ir18-Ir20, Ir20** displayed the best NADH photo-oxidation (TOF = 214 h^{-1}) *via* Figure 1.18b. **Ir20** displayed phototoxicities (400-700 nm, 17.2 J/cm^2) with IC_{50} values 1.2-3.3 nM against A549 and A549/DDP (cisplatin resistance) cancer cells. Notably, **Ir20** maintained its efficacy under hypoxic conditions, with IC_{50} values between 8.2-28 nM.[101]

In another study, Sadler and Huang group developed a series of D-glucose-appended cyclometalated Ir(III) photocatalysts, **Ir21-Ir23** (Figure 1.20).[102] The glucose pendant enhanced the aqueous solubility of **Ir21-Ir23**.[111,112] Additionally, the glucose moiety increased the cellular uptake inside the cancer cells due to the overexpression of GLUTs (glucose transporters) on cancer cell surfaces.[113] Aqueous solubility of **Ir23** was *ca.* 5 times higher than the related non-glycosylated complex **Ir24** (Figure 1.20). **Ir21-Ir23**

exhibited NADH/NAD(P)H oxidation potential *via* Figure 1.18b under light (465 nm, 11.7 J/cm^2).[102] **Ir23** showed the highest NADH/NAD(P)H photo-oxidation ability with a TON of 207.1/203.3 and TOF of 414.2/406.6 h^{-1}, respectively. **Ir21-Ir24** demonstrated anticancer activity in 2D cultures, with **Ir23** showing the highest photocytotoxicity index (PI=333.8) and an IC_{50} of *ca.* 0.08 µM against HeLa cells under 465 nm light. This superior performance of **Ir23** is attributed to its greater hydrophilicity than the other catalysts. **Ir23** also effectively damaged HeLa 3D multicellular tumor spheroids (*ca.* 400 µm) under light irradiation, showing activity in hypoxic cores.[102]

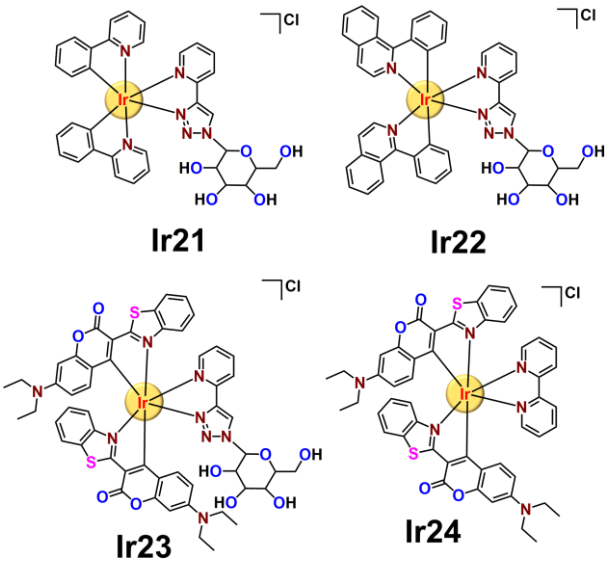

Figure 1.20: Structures of **Ir21-Ir24**.

Massaguer *et al.* explored the PCT activity of Ir(III)-photocatalysts (**Ir25-Ir27**) (Figure 1.21) to address the issue of cancer cell selectivity of the traditional photocatalysts.[103] In **Ir27**, Bombesin (BN) was appended for tumor recognition. BN is a 14-amino acid peptide (Pyr-Gln-Arg-Leu-Gly-Asn-Gln-Trp-Ala-Val-Gly-His-Leu-Met-NH_2) with a homologous seven-amino acid C-terminal region with GRP in ligands. Cancer cells often overexpress bombesin receptors such as the GRPR (Gastrin-Releasing Peptide Receptor).[114,115] The overexpression of these receptors allows selective binding of bombesin to cancer cells.[116] **Ir25-Ir27** induced NADH photo-oxidation, but TON or TOF was not provided.[103] The cellular uptake and phototoxicity study of **Ir25-Ir27** revealed that incorporating BN

significantly improved the selective accumulation and phototoxicity toward cancer cells.[103] This work indicated that the selective accumulation of photocatalysts in cancer cells could be improved by attaching tumor-targeting moieties like bombesin peptide.

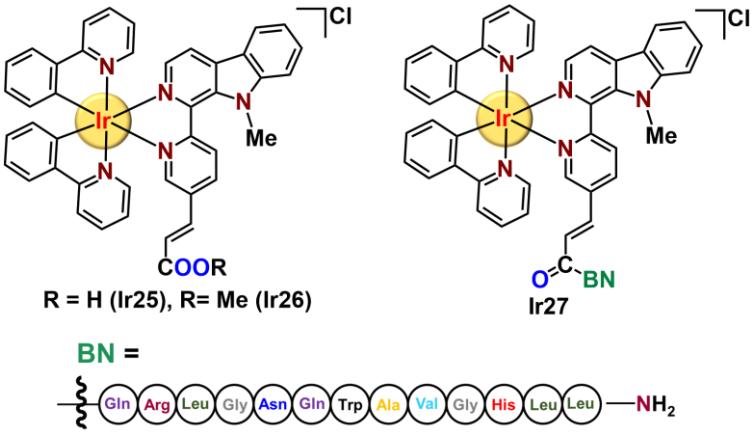

Figure 1.21: Structures of **Ir25-Ir27**.

1.7. Scope of Study and Objective of this Thesis

In the above section, we have discussed several Ir(III)-based photocatalysts, which highlights the scope of Ir(III) based photocatalysts in PCT. Even though these Ir(III)-based photocatalysts showed promising results in PCT, there is still a need to fix a few limitations. One of the key limitations of these photocatalysts is that they mainly absorb light in the low-wavelength region.[93-95,98-100] Like, Sadler *et al*. in their pioneering work on PCT, reported NADH oxidation under blue light irradiation (465 nm, 8.9 J cm^{-2}). Similarly, Huang, Ruiz, and Paira group also reported NADH oxidation under low-wavelength (blue light) light irradiation.[94,95,98-100] In general, blue light has a very limited penetration depth due to scattering and absorption by biological materials.[93-95,98-100] This restricts PCT's use to surface-level or shallow tumors, making it difficult to treat deeply seated tumors within

the body.[113,118] Moreover, it is worth noting that the photocatalytic NADH oxidation has mainly been quantified in solutions, and only one report is available showing alteration in the intracellular NADH/NAD^+ ratio.[93] The assessment and correlation of in-solution and in-cell NADH to NAD^+ photo-conversion would be valuable to understanding the photocatalytic anticancer effect of the photocatalysts in cancer cells.[93] Another crucial challenge with these photocatalysts is enhancing the NADH photo-oxidation efficiency of the photocatalysts. So far, most of the reported Ir(III) based photocatalysts had TOF in the *ca.* 17-400 h^{-1} range.[11] Increasing the NADH photo-oxidation TOF could also enhance the photo-cytotoxicity of the Ir(III)-photocatalysts.[11] The primary objective of this Ph.D. thesis is to design, synthesize, and characterize a novel Ir(III)-based photocatalysts capable of efficiently catalyzing the oxidation of NADH with a higher TON under biologically relevant conditions. Another objective of this thesis is the shifting of the absorption wavelength of the photocatalyst toward higher wavelengths with the help of a suitable choice of ligands. Additionally, we also tried to achieve light-triggered NADH oxidation inside the cancerous cell. Our choice of Ir(III)-based photocatalysts is based on, in particular, Ir(III) based complexes have shown significant advantages over many 3d/4d/5d metal-based complexes. These complexes exhibit high photostability, substantial Stokes shifts, and tunable emission colors.[119,120] These properties make Ir(III) photocatalysts effective in generating reactive oxygen species (ROS) under normoxic conditions, which is beneficial for therapeutic applications in cancer treatment.[119] Meanwhile, the choice of coumarin 6 shifted the absorption toward the green light region.[99,100] Also, it is fluorescent in nature, which tags the photocatalysts with fluorescent property, and these advantages can be used for cellular imaging to gain insight into the mechanism of photoinduced cell

death by monitoring the uptake and localization of the photocatalysts in cellular organelles.[99,100] Additionally, we have used phenanthroline and polypyridyl bases as ligands, as these moieties are known to be excellent photosensitizers that help the Ir(III)-based photocatalysts to achieve visible light-induced anticancer activity.[121]

1.8. References

1. K. E. Buckton, P. A. Jacobs, W. M. C. Brown, R. Doll, *Nature* **1962**, *193*, 591.
2. C. L. Chaffer, R. A. Weinberg, *Science* **2011**, *331*, 1559-1564.
3. S. A. Patel, P. Rodrigues, L. Wesolowski, S. Vanharanta, *Br. J. Cancer* **2020**, *124*, 3-12.
4. D. Hanahan, R. A. Weinberg, Cell **2011**, *44*, 646-674.
5. A. Agrawal, Y. Javanmardi, S. A. Watson, B. Serwinski, B. Djordjevic, W. Li, A. R. Aref, R. W. Jenkins, E. Moeendarbary, *npj. Biol. Phys. Mech.* **2025**, *2*, 3.
6. D. Hanahan, R. A. Weinberg, *Cell*, **2011**, *144*, 646-674.
7. S. Zhang, X. Xiao, Y. Yi, X. Wang, L. Zhu, Y. Shen, D. Lin, C. Wu, *Sig. Transduct. Target Ther.* **2024**, *9*, 149.
8. Z. Zhang, L. Zhou, N. Xie, E. C. Nice, T. Zhang, Y. Cui, C. Huang, *Sig. Transduct. Target Ther.* **2020**, *5*, 113.
9. R. Kurzrock, H. M. Kantarjian, A. S. Kesselheim, E. V. Sigal, *Nat. Rev. Clin. Oncol.* **2020**, *17*, 140–146.
10. H. Sung, J. Ferlay, R. L. Siegel, M. Laversanne, I. Soerjomataram, A. Jemal, F. Bray, *CA. Cancer J. Clin*. **2021**, *71*, 209-249.
11. A. K. Yadav, R. Kushwaha, A. A. Mandal, A. Mandal, S. Banerjee, *J. Am. Chem. Soc.* **2025**, *147*, 7161-7181.

12. J. J. Wilson, S. J. Lippard, *Chem. Rev.* **2014**, *114*, 4470-4495.

13. R. Baskar, K. A. Lee, R. Yeo, K. W. Yeoh, *Int. J. Med. Sci*. **2012**, *9*, 193-9.

14. R. Paprocka, M. W. Szadkowska, S. Janciauskiene, T. Kosmalski, M. Kulik, A. H. Basa, *Coord. Chem. Rev*. **2022**, *452*, 214307.

15. P. Štarha, R. Křikavová, *Coord. Chem. Rev*. **2024**, *501*, 215578.

16. H. Nelson, N. Petrelli, A. Carlin, J. Couture, J. Fleshman, J. Guillem, B. Miedema, D. Ota, D. Sargent, *J. Natl. Cancer Inst.* **2001**, *93*, 583-596.

17. N. Ogrinc, P. Saudemont, Z. Takats, M. Salzet, I. Fournier, *Trends. Mol. Med*. **2021**, *27*, 602-615.

18. J. Skliarenko, A. Barry, *Medicine*, **2020**, *48*, 84-89.

19. J. Bernier, E. J. Hall, A. Giaccia, *Nature* **2004**, *4*, 737-747.

20. M. He, S. Chen, H. Yu, X. Fan, H. Wu, Y. Wang, H. Wang, X. Yin, *iScience*, **2025**, *28*, 111602.

21. X. Qian, Y. Zheng, Y. Chen, *Adv. Mater*. **2016**, *28*, 8097-8129.

22. T. C. Johnstone, K. Suntharalingam, S. J. Lippard, *Chem. Rev.* **2016**, *116*, 3436–3486.

23. S. Ghosh, *Bioorg. Chem*. **2019**, *88*, 102925.

24. S. Dasari, P. B. Tchounwou, *Eur. J. Pharmacol*. **2014**, *740*, 364-378.

25. R. G. Jones, J. Grainger, M. Harrison, P. Ostler, A. Makris, *Br. J. Cancer*, **2006**, *94*, 363-371.

26. L. Best, P. Simmonds, C. Baughan, R. Buchanan, C. Davis, I. Fentiman, S. George, M. Gosney, J. Northover, C. Williams, *Cochrane Database Syst. Rev*. **2000**, *24*, 2000.

27. P. D. O. Dowd, D. F. Sutcliffe, D. M. Griffith, *Coord. Chem. Rev*. **2023**, *497*, 215439.

28. J. L. Nitiss, *Nat. Rev. Cancer*. **2009**, *9*, 338-350.

29. S. Bonnet, *Dalton Trans*. **2018**, *47*, 10330-10343.

30. X. Su, X. Zhou, C. Xiao, W. Peng, Q. Wang, Y. Zheng, *Front. Oncol*. **2022**, https://doi.org/10.3389/fonc.2022.750970.

31. D. A. Gewirtz, *Biochem. Pharmacol*. **1999**, *57*, 727-741.

32. Y. Pommier, E. Leo, H. Zhang, C. Marchand, *Chem. Biol*. **2010**, *17*, 421-433.

33. D. B. Longley, D. P. Harkin, P. G. Johnston, *Nat. Rev. Cancer*. **2003**, *3*, 330-338.

34. R. Seigers, J. E. Fardell, *Neurosci. Biobehav. Rev*. **2011**, *35*, 729-741.

35. M. E. Richardson, D. W. Siemann, *Cancer Res.* **1995**, *55*, 1691-1695.

36. S. Mazzaferro, K. Bouchemal, G. Ponchel, *Drug Discov. Today*, **2013**, *18*, 25-34.

37. L. Kelland, *Nat. Rev. Cancer* **2007**, *7*, 573-584.

38. S. Rottenberg, C. Disler, P. Perego, *Nat. Rev. Cancer* **2020**, *21*, 37-50.

39. B. Rosenberg, L. VanCamp, T. Krigas, *Nature* **1965**, *205*, 698.

40. J. Karges, T. Yempala, M. Tharaud, D. Gibson, G. Gasser, *Angew. Chem. Int. Ed.* **2020**, *59*, 7069-7075.

41. N. J. Wheate, S. Walker, G. E. Craiga, R. Oun, *Dalton Trans.* **2010**, *39*, 8113-8127.

42. N. P. E. Barry, P. J. Sadler, *Chem. Commun.* **2013**, *49*, 5106-5131.

43. U. Anand, A. Dey, A. K. S. Chandel, R. Sanyal, A. Mishra, D. K. Pandey, V. D. Falco, A. Upadhyay, R. Kandimalla, A. Chaudhary, J. K. Dhanjal, S. Dewanjee, J. Vallamkondu, J. M. P. D. L. Lastra, *Genes Dis*. **2023**, *10*, 1367-1401.

44. J. Crawford, D. Herndon, K. Gmitter, J. Weiss, *Future Oncol*. **2024**, *20*, 1515-1530.

45. S. P Vaidya, S. Gadre, R. T. Kamisetti, M. Patra, *Biosci. Rep.* **2022**, *42*, BSR20212160.

46. A. F. Martinez, J. Shapiro, S. Goldfarb, J. Nangia, J. J. Jimenez, R. Paus, M. E. Lacouture, *J. Am. Acad. Dermatol*. **2018**, *80*, 1179-1196.

47. Z. H. Siddik, *Oncogene* **2003**, *22*, 7265-7279.

48. A. M. Florea, D. Büsselberg, *Cancers*, **2011**, *3*, 1351-1371.

49. B. Bahrami, M. H. Farsangi, H. Mohammadi, E. Anvari, G. Ghalamfarsa, M. Yousefi, F. J. Niaragh, *Immunol. Lett*. **2017**, *190*, 64-83.

50. E. P. Herrero, A. F. Medarde, *Eur. J. Pharm. Biopharm*. **2015**, *93*, 52-79.

51. S. Bonnet, *J. Am. Chem. Soc.* **2023**, *145*, 23397-23415.

52. N. A. Kratochwil, Z. Guo, P. D. S. Murdoch, J. A. Parkinson, P. J. Bednarski, P. J. Sadler, *J. Am. Chem. Soc*. **1998**, *120*, 8253-8254.

53. L. A. Emens, *Cancer J*. **2010**, *16*, 295.

54. R. Bagherifar, S. H. Kiaie, Z. Hatami, A. Ahmadi, A. Sadeghnejad, B. Baradaran, R. Jafari, Y. Javadzadeh, *J. Nanobiotechnol.* **2021**, *19*, 110.

55. K. S Rallis, T. H. L. Yau, M. Sideris, *Anticancer Res*. **2021**, *41*, 1-7.

56. S. Saha, R. Kushwaha, A. Mandal, N. Singh, S. Banerjee, *Coord. Chem. Rev.* **2025**, *525*, 216306.

57. L. K. McKenzie, H. E. Bryant, J. A. Weinstein, *Coord. Chem. Rev*. **2019**, *379*, 2-29.

58. T. C. Pham, V. N. Nguyen, Y. Choi, S. Lee, J. Yoon, *Chem. Rev.* **2021**, *121*, 13454-13619.

59. D. E. J. G. J. Dolmans, D. Fukumura, R. K. Jain, *Nat. Rev. Cancer* **2003**, *3*, 380-387.

60. X. Zhao, J. Liu, J. Fan, H. Chao, X. Peng, *Chem. Soc. Rev.* **2021**, *50*, 4185-4219.

61. W. Fan, P. Huang, X. Chen, *Chem. Soc. Rev.* **2016**, *45*, 6488-6519.

62. B. Kar, U. Das, N. Roy, P. Paira, *Coord. Chem. Rev.* **2023**, *474*, 214860.

63. Y. Wu, S. Li, Y. Chen, W. He, Z. Guo, *Chem. Sci.* **2022**, *13*, 5085.

64. J. P. Celli, B. Q. Spring, I. Rizvi, C. L. Evans, K. S. Samkoe, S. Verma, B. W. Pogue, T. Hasan, *Chem. Rev.* **2010**, *110*, 2795-2838.

65. J. F. Lovell, T. W. B. Liu, J. Chen, G. Zheng, *Chem. Rev.* **2010**, *110*, 2839-2857.

66. J. Xu, J. Gao, Q. Wei, *J. Nanomater*, **2016**, *7*, 8507924.

67. M. Ethirajan, Y. Chen, P. Joshi, R. K. Pandey, *Chem. Soc. Rev.* **2011**, *40*, 340-362.

68. A. Kamkaew, S. H. Lim, H. B. Lee, L. V. Kiew, L. Y. Chung, K. Burgess, *Chem. Soc. Rev.* **2013**, *42*, 77-88.

69. J. Zhao, W. Wu, J. Sun, S. Guo, *Chem. Soc. Rev.* **2013**, *42*, 5323-5351.

70. L. Liang, W. Wang, M. Li, Y. Xu, Z. Lu, J. Wei, B. Z. Tang, F. Sun, R. Tong, *ACS Appl. Mater. Interfaces* **2025**, *17*, 16668-16680.

71. W. Zhao, L. Wang, M. Zhang, Z. Liu, C. Wu, X. Pan, Z. Huang, C. Lu, G. Quan, *MedComm*. **2024**, *5*, e603.

72. M. Lan, S. Zhao, W. Liu, C. S. Lee, W. Zhang, P. Wang, *Adv. Healthcare Mater.* **2019**, *8*, 1900132.

73. M. R. Hamblin, *Photochem Photobiol*. **2020**, *96*, 506-516.

74. A. E. O. Connor, W. M. Gallagher, A. T. Byrne, *Photochem. Photobiol*. **2009**, *85*, 1053-1074.

75. E. D. Sternberg, D. Dolphin, *Tetrahedron*, **1998**, *54*, 4151-4202.

76. S. M. K. L. Colón, H. Yin, J. Roque III, P. Konda, S. Gujar, R. P. Thummel, L. L. C. G. Cameron, S. A. McFarland, *Chem. Rev*. **2019**, *119*, 797-828.

77. C. K. Prier, D. A. Rankic, D. W. C. MacMillan. *Chem. Rev*. **2013**, *113*, 5322-5363.

78. J. H. Shon, D. Kim D, M. D. Rathnayake, S. Sittel, J. Weaver, T. S. Teets, *Chem. Sci*. **2021**, *12*, 4069-4078.

79. Y. Yao, C. L. Hou, Z. S. Yang, G. Ran, L. Kang, C. Li, W. Zhang, J. Zhang, J. L. Zhang, *Chem. Sci*. **2019**, *10*, 10170-10178.

80. W. Sun, S. Li, B. Häupler, J. Liu, S. Jin, W. Steffen, U. S. Schubert, H. J. Butt, X. J. Liang, S. Wu, *Adv. Mater.* **2017**, *29*, 1603702.

81. Z. Lv, H. Wei, Q. Li, X. Su, S. Liu, K. Y. Zhang, W. Lv, Q. Zhao, X. Li, W. Huang, *Chem. Sci.* **2018**, *9*, 502.

82. W. Wu, D. Mao, F. Hu, S. Xu, C. Chen, C. J. Zhang, X. Cheng, Y. Yuan, D. Ding, D. Kong, *Adv. Mater.* **2017**, *29*, 1700548.

83. C. Jin, F. Liang, J. Wang, L. Wang, J. Liu, X. Liao, T. W. Rees, B. Yuan, H. Wang, Y. Shen, Z. Pei, L. Ji, H. Chao, *Angew. Chem., Int. Ed.* **2020**, *59*, 15987.

84. S. A. McFarland, A. Mandel, R. D. White, G. Gasser, *Curr. Opin. Chem. Biol*. **2020**, *56*, 23-27.

85. J. An, S. Tang, G. Hong, W. Chen, M. Chen, J. Song, Z. Li, X. Peng, F. Song, W. H. Zheng, *Nat Commun* **2022**, *13*, 2225.

86. I. S. Turan, D. Yildiz, A. Turksoy, G. Gunaydin, E. U. Akkaya, *Angew. Chem. Int. Ed.* **2016**, *55*, 2875.

87. Y. Liu, Y. Liu, W. Bu, C. Cheng, C. Zuo, Q. Xiao, Y. Sun, D. Ni, C. Zhang, J. Liu, J. Shi, *Angew. Chem. Int. Ed*. **2015**, *54*, 8105-8109.

88. D. V. Titov, V. Cracan, R. P. Goodman, J. Peng, Z. Grabarek, V. K. Mootha, NAD^+/NADH ratio. *Science,* **2016**, *352*, 231-235.

89. M. Li, K. H. Gebremedhin, D. Ma, Z. Pu, T. Xiong, Y. Xu, J. S. Kim, X. Peng, *J. Am. Chem. Soc*. **2022**, *144*, 163-173.

90. X. Wang, J. Peng, C. Menga, F. Feng, *Chem. Sci.* ***2024***, *15*, 12234-12257.

91. Z. Zhu, L. Wei, A. K. Yadav, Z. Fan, A. Kumar, M. Miao, S. Banerjee, H. Huang, *J. Org. Chem.* **2023**, *88*, 626-631.

92. S. Banerjee, P.J. Sadler, *RSC Chem. Biol.* **2021**, *2*, 12-29.

93. H. Huang, S. Banerjee, K. Qiu, P. Zhang, O. Blacque, T. Malcomson, M. J. Paterson, G. J. Clarkson, M. Staniforth, V. G. Stavros, G. Gasser, H. Chao, P. J. Sadler, *Nat. Chem*. **2019**, *11*, 1041-1048.

94. J. Kasparkova, G. A. Hernández, H. Kostrhunova, M. Goicuría, V. Novohradsky, D. Bautista, L. Markova, M. D. Santana, V. Brabec, J. Ruiz, *J. Med. Chem*. **2024**, *11*, 691-708.

95. Z. Fan, Y. Rong, T. Sadhukhan, S. Liang, W. Li, Z. Yuan, Z. Zhu, S. Guo, S. Ji, J. Wang, R. Kushwaha, S. Banerjee, K. Raghavachari, H. Huang, *Angew. Chem. Int. Ed*. **2022**, *61*, e202202098.

96. M. Shee, J. Schleisiek, N. Maity, G. Das, N. Montesdeoca, M. H. H. Thi, K. R. Gore, J. Karges, N. D. P. Singh, *Small* **2025**, *21*, 2408437.

97. Y. Yang, Y. Gao, J. Zhao, S. Gou, *Inorg. Chem. Front*. **2024**, *11*, 436-450.

98. U. Das, P. Paira, *Dalton Trans*. **2024**, *53*, 6459-6471.

99. C. Huang, C. Liang, T. Sadhukhan, S. Banerjee, Z. Fan, T. Li, Z. Zhu, P. Zhang, K. Raghavachari, H. Huang, *Angew. Chem. Int. Ed.* **2021**, *60*, 9474-9479.

100. Z. Fan, J. Xie, T. Sadhukhan, C. Liang, C. Huang, W. Li, T. Li, P. Zhang, S. Banerjee, K. Raghavachari, H. Huang, *Chem. Eur. J*. **2022**, *28*, e202103346.

101. L. Wei, R. Kushwaha, A. Dao, Z. Fan, S, Banerjee, H. Huang, *Chem. Commun.* **2023**, *59*, 3083-3086.

102. Z. Zhu, L. Wei, Y. Lai, W. L. O. Carter, S. Banerjee, P. J. Sadler, H. Huang, *Dalton Trans.* **2022**, *51*, 10875-10879.

103. J. S. Villafruela, C. B. Casadesús, G. R. Llach, M. Iglesias, M. M. Alonso, M. Planas, L. Feliu, G. Espino, A. Massaguer, *Inorg. Chem.* **2024**, *63*, 19140-19155.

104. S. Wei, H. Liang, A. Dao, Y. Xie, F. Cao, Q. Ren, A. K. Yadav, R. Kushwaha, A. A. Mandal, S. Banerjee, P. Zhang, S. Ji, H. Huang, *Sci. China Chem.* **2023**, *66*, 1482-1488.

105. A. A. Mandal, V. Singh, S. Saha, S. Peters, T. Sadhukhan, R. Kushwaha, A. K. Yadav, A. Mandal, A. Upadhyay, A. Bera, A. Dutta, B. Koch, S. Banerjee, *Inorg. Chem.* **2024**, *63*, 7493-7503.

106. Z. Fan, J. Xie, R. Kushwaha, S. Liang, W. Li, A. A. Mandal, L. Wei, S. Banerjee, H. Huang, *Chem. Asian J.* **2023**, *18*, e202300047.

107. A. Dao, S. Chen, L. Pan, Q. Ren, X. Wang, H. Wu, Q. Gong, Z. Chen, S. Ji, J. Ru, H. Zhu, C. Liang, P. Zhang, H. Xia, H. Huang, *Adv. Healthc. Mater.* **2024**, *13*, 2400956.

108. Lu, N.; Deng, Z.; Gao, J.; Liang, C.; Xia, H.; Zhang, P. An osmium-peroxo complex for photoactive therapy of hypoxic tumors. *Nat. Commun.* **2022**, *13*, 2245.

109. G. V. S. Moreno, D. H. Romero, O. G. Barradas, O. V. Vera, S. R. Luna, C. A. C. Cruz, A. L. Monteon, J. C. Ahumada, D. M. Morales, R. C. Peralta, *Coord. Chem. Rev.* **2022**, *472*, 214790.

110. P. Weerasinghe, L. M. Buja, *Exp. Mol. Pathol.* **2012**, *93*, 302-308.

111. H. Martin, L. R. Lazaro, T. Gunnlaugsson, E. M. Scanlan, *Chem. Soc. Rev.* **2022**, *51*, 9694-9716.

112. J. Liu, X. Liao, K. Xiong, S. Kuang, C. Jin, L. Ji, H. Chao, *Chem. Commun.* **2020**, *56*, 5839-5842.

113. M. Patra, S. G. Awuah, S. J. Lippard, *J. Am. Chem. Soc.* **2016**, *138*, 12541-12551.

114. P. Moreno, I. R. Alvarez, T. W. Moody, R. T. Jensen, *Expert Opin. Ther. Targets* **2016**, *20*, 1055-1073.

115. D. Pooja, A. Gunukula, N. Gupta, D. J. Adams, H. Kulhari, *Int. J. Biochem. Cell Biol.* **2019**, *114*, 105567.

116. L. Baratto, H. Jadvar, A. Iagaru, *Mol. Imaging Biol.* **2018**, *20*, 501-509.

117. L. Wei, R. Kushwaha, T. Sadhukhan, H. Wu, A. Dao, Z. Zhang, H. Zhu, Q. Gong, J. Ru, C. Liang, P. Zhang, S. Banerjee, H. Huang, *J. Med. Chem.* **2024**, *67*, 11125-11137.

118. Z. Wang, L. Wei, J. Lin, C. Huang, H. Chen, D. Fan, W. Hu, J. Liu, H. Huang, Z. Wang, X. Wang, *J. Med. Chem.* **2024**, *67*, 13435-13445.

119. H. Huang, S. Banerjee, P. J. Sadler, *ChemBioChem* **2018**, *19*, 1574.

120. P. Szymaszek, M. T. Czochara, J. Ortyl, *Eur. J. Med. Chem*. **2024**, *276*, 116648.

121. A. Dao, H. Wu, S. Wei, H. Huang, *Phys. Chem. Chem. Phys*. **2023**, *25*, 20001-20008.